BACHELOR

Modelling of acoustic metamaterials for ultrasound imaging applications

Robdon, K. (Houssein)

Award date:
2024

Bachelor's Final project

Modelling of acoustic metamaterials for ultrasound imaging applications

Quartile 1-2 - 2023/2024

Mechanics of Materials

Full Name	Student ID	Study
Houssein Robdon	0952818	Mechanical Engineering

Supervised by Georgia Kuci, Varvara Kouznetsova

Eindhoven, February 26, 2024

Contents

List of Symbols

Symbol	Definition	Unit
P	Pressure	Pa (Pascal)
u	Displacement	m (meter)
ρ	Density	kg/m^3 (kilogram per cubic meter)
t	Time	s (second)
m	Mass	kg (kilogram)
q	Wavenumber	m^-1 (per meter)
ω	Angular frequency	rad/s (radian per second)
L	Lattice constant	m (meter)
F	Force	N (Newton)
k	Spring stiffness	N/m (Newton per meter)
σ	Stress	Pa (Pascal)
θ	Angle	rad (radian)
c	Wave speed	m/s (meter per second)
l	Length	m (meter)
Z	Impedance	Rayl
g	Real part of wavenumber	m^-1 (per meter)
h	Imaginary part of wavenumber	m^-1 (per meter)
β	Mass ratio	(dimensionless)
α	Stifness ratio	(dimensionless)
$\|R\|$	Reflection magnitude	(dimensionless)
B	complex wave amplitude	(dimensionless)

List of symbols

1 Introduction

Ultrasound imaging guidance has developed in the medical world, providing real-time visualization of the needle inside the body. This technology works by using a transducer, also known as probe, for generating and receiving the acoustic waves that create the ultrasound image. However, a challenge in this field has been to consistently visualize the needle during the ultrasound procedures. A continuous visualization of the needle is important to prevent any inaccuracies and complications.
Needles used in ultrasound imaging procedures have a coating specifically designed to provide the reflection of acoustic waves, thereby enabling the visibility of the needle in ultrasound images. This coating is not merely a simple layer of material applied to the needle. Instead, it's a complex structure engineered to interact with acoustic waves. Recent developments in materials science have introduced a promising solution to the challenge of maintaining continuous needle visualization, with improving the needle's coating."

Figure 1: Needle visualization with ultrasound imaging [1]

The coating is made up of a locally resonant acoustic metamaterial(LRAM), which is a distinct category of artificially structured materials with the ability to manipulate acoustic waves. The manipulation of acoustic waves is achieved through the careful design and arrangement of the material's internal structure. Figure 2 shows an acoustic metamaterial consisting of different unit cells with heavy inclusions surrounded by a compliant layer. When an acoustic wave encounters the LRAM, it interacts with the internal components causing the inclusions to vibrate or resonate. This resonance can then influence the magnitude of the reflected wave. By carefully designing the material's structure, it's possible to control these resonances and therefore control the behavior of the reflected wave.

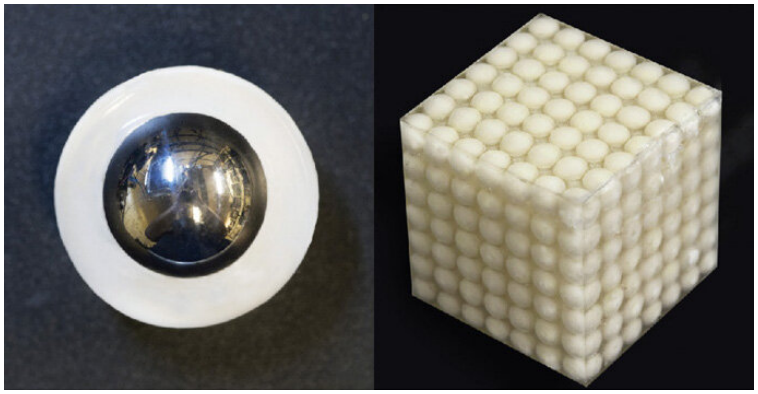

Figure 2: Acoustic metamaterial: Left single lead inclusion with compliant layer . Right structure of multiple unit cells [2]

The LRAM is able dictate how much of an acoustic wave is reflected and at what angle, much like how a mirror controls the reflection of light. This control even extends to negative angles, where waves are redirected back to the probe. This unique characteristic is not inherent in natural materials, making LRAMs a subject of intense scientific interest. The potential applications of LRAMs have broadened and are used in the medical field, where they are used in the development of new coatings for medical devices [2].
Another remarkable property of LRAMs is their ability to exhibit band gaps. Band gaps are specific frequency ranges where wave propagation is attenuated or stopped completely. When waves can't propagate they will be reflected back. A band gap is created due to its local resonance mechanism located within the material's structure. The presence of band gaps provides the capability for users to locally manipulate the magnitude of the reflection of an incoming wave.

Dispersion plots are often used to analyze these band gaps. These plots graphically depict the relationship between frequency and the wave number. By studying these plots it's possible to gain insights into the frequency ranges within the material and understand how the structure of the material influences these ranges.

This document presents the objectives and structure of an ongoing project that is centered around the design and optimization of a LRAM coating. The initial design of this innovative coating has already shown promising results, with a significant increase in the reflection magnitude and the achievement of a negative reflection angle. However, these preliminary results were obtained through simulations that require substantial computational resources and time. This presents a challenge for realistic designs as the computational demands make it both difficult and costly.

As we progress through the stages of the project, we will transition to using a one-dimensional discrete model. This approach simplifies the problem, making it more manageable and less computationally intensive.
The project involves a detailed investigation into how various geometric and material parameters influence the performance of the LRAM.

The performance of the LRAM will be analyzed in terms of its reflection magnitude and the band gap. Reflection magnitude refers to the proportion of incident acoustic wave that is reflected by the LRAM, while the band gap is the range of frequencies for which propagation is forbidden in the LRAM. These are critical parameters that determine the effectiveness of the LRAM in enhancing needle visualization.

A good performance result would be a high reflection magnitude, meaning that a large proportion of the incident acoustic wave is reflected back. A wide band gap is desirable as it means that the LRAM can effectively block a broad range of frequencies, improving its performance.

The influence of geometric and material parameters on the performance of the LRAM coating will be analyzed with help of dispersion plots and the reflection coefficient. This analysis will guide the optimization of the LRAM design. Understanding these relationships is crucial as it enables the optimization of the needle's coating for enhanced reflection, thereby improving needle visualization, safety and success rate of ultrasound imaging procedures.

2 Locally resonant acoustic metamaterials

Locally Resonant Acoustic Materials (LRAM) were first introduced with an unique three-component structure, often referred to as the hard-soft-hard configuration [3]. This structure is characterized by a heavy core which is one of its most important properties. The structure of the LRAM is composed of a spherical lead inclusion, which forms the 'hard' core of the structure. This lead inclusion is surrounded by a 'soft' coating made of rubber, providing a contrast in material properties that is essential for the functioning of the LRAM. This hard-soft combination is then embedded within an epoxy matrix forming the second 'hard' component of the structure.

In figure 3a , a cross-sectional view of this structure is presented in a schematic representation. This diagram provides a visual understanding of the arrangement and interaction of the different components within the LRAM. The matrix itself has a rigid structure which is crucial for its acoustic properties. The presence of a soft coating around the heavy core facilitates the independent movement of the heavier inclusions separate from the surrounding matrix material. This phenomenon is particularly noticeable when the material is subjected to excitation at specific resonant frequencies, resulting in a relative motion between the inclusions and the matrix material. This dynamic behavior is directly related to the special characteristics of the local resonant acoustic materials.

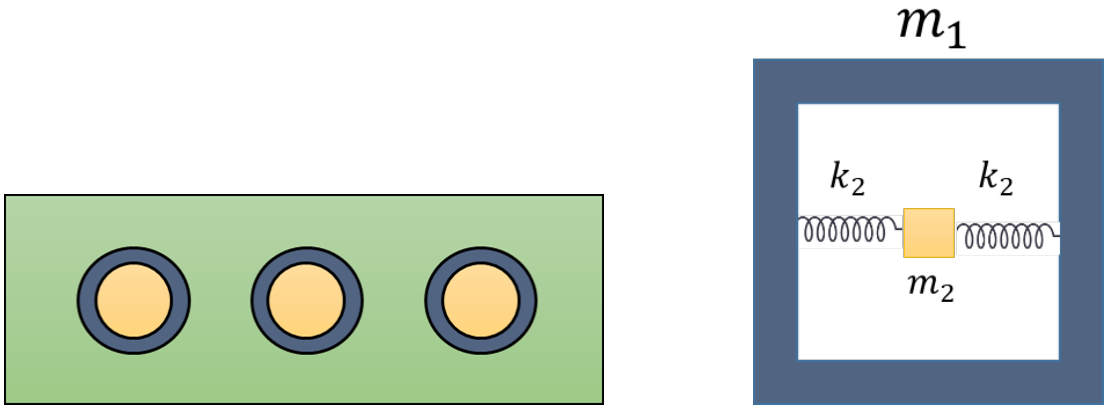

(a) Cross section of metamaterial with a heavy core surrounded by a compliant layer in a rigid matrix

(b) 1D-model of one inclusion connected to springs with the matrix

Figure 3: Cross section (Left) and 1D model (right)

To better understand and visualize the behavior of this acoustic material, a one-dimensional model known as the discrete mass-spring system is introduced. In the discrete mass-spring system, each mass represents a physical body and each spring represents the force between bodies as depicted in figure 3b. For the metamaterial, the heavy inclusions are represented by the discrete mas m_2 and m_1 for the matrix. The springs k_2 can be thought of as the compliant layer. The springs in the system represent the forces between the masses, which in this case are the interactions between the heavy inclusions and the soft coating. The elasticity of the springs corresponds to the flexibility of the compliant layer. In this manner a discrete system that accurately represents the metamaterial is presented.

In composite structures, such as metamaterials, the mass density is represented as the volume-averaged density of all separate components. This implies that the total mass of all the components is divided by the total volume they occupy, yielding an average density for the entire structure. For a system composed of two elements, this can be represented as $Dv = fD_1 + (1-f)D_2$, where D_1 and D_2 are the densities of the matrix material (component 1) and the inclusions (component 2), and f is the volume fraction of the inclusions [5]. This equation assumes that all components of the composite move together. However, at certain resonant frequencies the inclusions can move out of phase with the matrix material. "Out of phase" means that while the matrix material might be moving in one direction, the inclusions could be moving in the opposite direction. This invalidates the static mass density law and can lead to a negative effective mass density [6].
The concept of the effective mass provides a unified approach to handle the combined system of the inclusion and the matrix, rather than treating them as separate entities. This implies that the entire mass can be represented by a single term the effective mass, as $m_{\text{eff}} = \rho_{\text{eff}} V$. The effective mass is defined as the ratio of the force F acting on the unit cell to the product of the negative square of the angular frequency $-\omega^2$ and the displacement u_1 of the unit cell. This definition is derived from Newton's second law and mathematically this is presented as:

$$\rho_{\text{eff}} V = \frac{F}{-\omega^2 u_1} \tag{1.1}$$

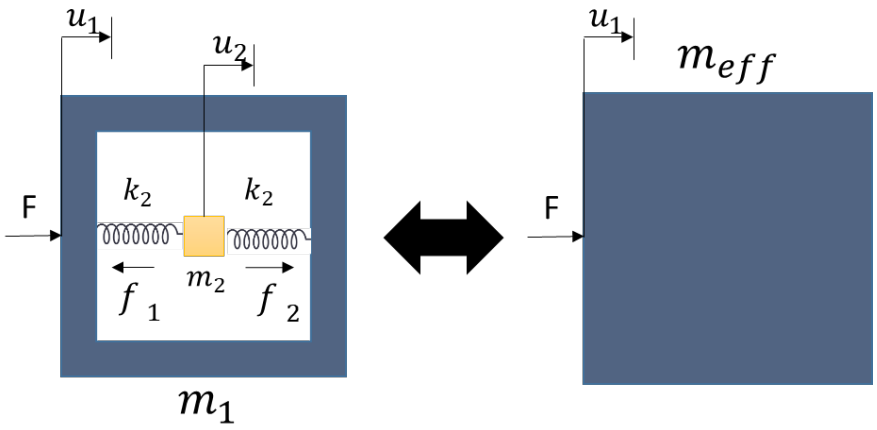

Figure 4: Consolidation phase where two masses are represented as an effective mass

To better understand how these acoustic metamaterial behave at specific frequencies and their operational principle , let's consider a single inclusion connected to the matrix material, as depicted in figure 4.This basic unit can be modeled as a rigid frame of mass m_1 with a cavity containing a rigid cube m_2 connected by two massless and elastic springs with stiffness K_2 on both sides of mass m_2 . Using Hooke's law, the forces acting on the rigid frame can be described. If f_1 and f_2 are denoted as the forces exerted by the left and right spring, respectively, and u_1 as the displacements of the frame and u_2 as the displacement of the cube, the net force acting on the rigid cube is given by:

$$-f_1 + f_2 = 2K_2(u_1 - u_2) \tag{1.2}$$

Equation 1.2 tells us that the net force on the cube is proportional to the difference in displacement between the frame and the cube. The cube and frame are moving out of phase when the difference is non-zero.

Furthermore, by rewriting Newton's second law for the mass-spring system excited by a simple harmonic motion, we obtain:

$$m_2\ddot{u_2} = -f_1 + f_2 = (-i\omega)^2 m_2 u_2 \tag{1.3}$$

A relationship between the displacements u_1 of the matrix material and the cube (resonator) u_2 can be derived as:

$$u_2 = \frac{2K_2}{2K_2 - m_2\omega^2} u_1 \tag{1.4}$$

This equation illustrates the relationship between the displacement of the cube u_2 and the displacement of the frame u_1 at a given frequency ω.

With an external force F, Newton's second law is applied to the rigid frame in the same manner to obtain the following result:

$$F + f_1 - f_2 = (-i\omega)^2 m_1 u_1 \tag{1.5}$$

Substituting $-f_1 + f_2$ from equation 1.3, the equation can further be rearranged to:

$$F = (-i\omega)^2 [m_1 u_1 + m_2 u_2] \tag{1.6}$$

It shows that the external force F is equal to the sum of the forces acting on the rigid frame and the cube.

A new expression for the effective mass is derived when force F as equation 1.6 is substituted into the effective mass equation 1.1, The new expression is denoted as:

$$\rho_{eff} V = m_1 + m_2 \frac{u_2}{u_1} \tag{1.7}$$

Finally substituting equation 1.4 for u_2 results in a relationship for the frequency-dependent effective mass [7]:

$$M_{eff} = \rho_{eff} V = m_1 + \frac{m_2 \cdot 2K_2}{2K_2 - m_2\omega^2} = m_1 + \frac{m_2\omega_0^2}{\omega_0^2 - \omega^2} \tag{1.8}$$

Where $\omega_0 = \sqrt{\frac{2k_2}{m_2}}$, is the local resonance frequency of m_2. The effective mass is a function of $\frac{\omega_0^2}{\omega^2}$ and is highly influenced by the local resonance frequency ω_0.

Interestingly, as the forcing frequency ω approaches ω_0 from a higher value the effective mass turns negative, and if the forcing frequency ω becomes equal to the resonance frequency ω_0, the effective mass turns infinite. If the mass turns negative according to Newton's second law of motion, the acceleration would oppose the applied force leading to a reduction in the response amplitude [8].

The emergence of a negative effective mass is a consequence of the attempt to represent a two-mass system with a single mass. Each mass responds independently to an applied force. The two masses are able to move out of phase, it's as if one mass is moving forward while the other is moving backward making the system behave as if it has a negative effective mass. So when we represent a system with a single effective mass , interactions between the two masses can lead to a negative effective mass [9].

3 Dispersion relation

In the study of metamaterial understanding the dispersion relation is crucial. The dispersion relation reveals the relationship between the frequency and the wavenumber of a wave propagating through the system. This is particularly important because it provides insight into how waves of different frequencies propagate at different speeds, leading to a phenomenon known as dispersion.
Following this, we delve into the arrangement of the unit cells in the composite structure called the lattice system. Here, we consider a series of effective masses interconnected by springs with a stiffness denoted as k_1. These unit cells are arranged periodically with a spacing of L seen in figure5. This approach simplifies the system by focusing on the effective mass, rather than treating the inner and outer masses separately. It's crucial to ensure that the resulting dispersion relation remains unchanged compared to the result where you deal with the two masses individually. This ensures that the system is not affected due to the simplification with the effective masses .

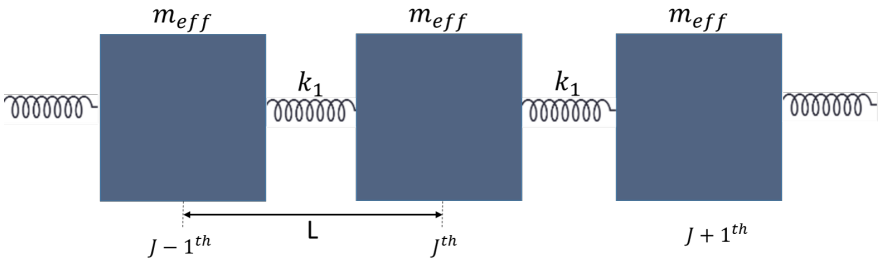

Figure 5: 1D infinite structure of effective masses connected by springs denoted as k_1

The equation of motion in this lattice structure with effective masses is represented as:

$$M_{\text{eff}}\frac{d^2U_y^{(j)}}{dt^2} = k_1(U_y^{(j+1)} - U_y^{(j)}) - k_1(U_y^{(j)} - U_y^{(j-1)}) = k_1(U_y^{(j+1)} - 2U_y^{(j)} + U_y^{(j-1)}) \tag{3.1}$$

Where, M_{eff} denotes the effective mass of the unit cells, k_1 represents the springs connecting the unit cells and $U_y^{(j)}$ signifies the displacement of the j^{th} unit cell. The terms $U_y^{(j-1)}$ and $U_y^{(j+1)}$ are the displacements of the neighboring unit cells. The displacement of the j^{th} unit cell is considered relative to both neighboring unit cells in the equation of motion, which is why it is present two times and given by $-2U_y^{(j)}$ in the equation . The term y is used to distinguish between the displacement of the resonator and the outer mass. However, since the effective mass is being considered, the distinction becomes irrelevant. The focus lies in understanding the propagation of waves within the lattice structure. In order to achieve this, the focus is on seeking the solutions for displacement $U_y^{(j)}$.

The harmonic wave solution for the jth unit cell is:

$$u_y^{(j)} = B_y e^{i(nqL-\omega t)} \tag{3.2}$$

with B_y the complex wave amplitude, q the wavenumber, ω the angular frequency and L the lattice constant. By substituting equation 3.2 into equation 3.1 and simplifying, a relationship between the frequency ω and the wave number q is derived:

$$\omega^2 = -\frac{k_1}{M_{\text{eff}}}\left(e^{iqL} - e^{-iqL}\right) \tag{3.3}$$

The relationship identified, referred as the dispersion relation, serves as a basis for constructing relevant dispersion graphs. Using trigonometric identities the relation can be further simplified as:

$$\omega^2 = \frac{2k_1(1-\cos(qL))}{M_{\text{eff}}} \tag{3.4}$$

Equation 3.4 gives the relation between ω and qL for the effective mass. For the same system but with unit cells having two distinct masses it is known that the dispersion relation must be the same. Therefore the dispersion relation from the mass-in-mass system can be utilized to chose the m_{eff} which maintains the consistency of the dispersion relation.

Now let's consider an infinite series of two mass system with m_2 and m_1 for the inner and outer mass respectively. The outer masses m_1 are connected by springs k_1. Each inner mass m_2 is connected to its corresponding outer mass m_1 in the same unit cell by spring k_2. The infinitely long one-dimensional lattice system composed of mass-in-mass lattice points, is shown in figure 6. The construction of this lattice system is achieved by connecting the unit cells, as shown in figure 3b. with linear springs. In this system, the springs k_1 represent the connections and interactions between the matrix materials of adjacent unit cells.

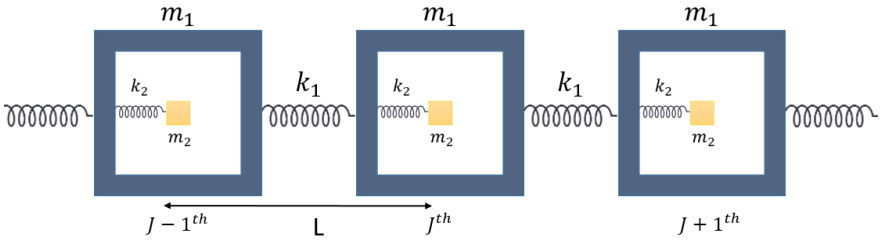

Figure 6: 1D infinite structure of mass-in-mass system

The focus is now on wave propagation within the mass-in-mass lattice structure, instead of solely focusing on u_y both masses are treated separately. Seeking harmonic wave solutions that describe the displacements of both u_1 for the outer mass, and u_2 for the resonator.

The equations of motion for the j-th unit cell for the mass-in-mass lattice are as follow:

for the outer mass

$$m_1^{(j)}\frac{d^2u_1^{(j)}}{dt^2} + k_1(2u_1^{(j)} - u_1^{j-1} - u_1^{j+1}) = k_2(u_1^{(j)} - u_2^{(j)}) = 0 \tag{3.5}$$

and for the inner mass

$$m_2^{(j)}\frac{d^2u_2^{(j)}}{dt^2} + k_2(u_2^{(j)} - u_1^{(j)}) = 0 \tag{3.6}$$

The harmonic wave solution for the j^th unit cell aligns with the harmonic wave used before, as shown in equation 3.2. With $u_1^{(j)} = B_1e^{i(nqL-\omega t)}$ for the outer mass and $u_2^{(j)} = B_2e^{i(nqL-\omega t)}$ for the resonator. The dispersion relation is accomplished by substituting the harmonic wave solution into equations 3.5 and 3.6. With these two equations, the dispersion relation is derived as:

$$(M_1m_2)\omega^4 - (M_1 + m_2)k_2 + 2M_1k_1(1 - \cos(qL))\omega^2 + k_1k_2(1 - \cos(qL)) = 0 \tag{3.7}$$

The dispersion relation, as derived above provides a mathematical relation that makes it possible to understand the relationship between the frequency ω and the wave number q of the system . These relations are particularly useful when visualized graphically.

3.1 Dispersion curves

Utilizing the dispersion relation from Equation 3.7, two branches of the band structure are generated. The corresponding dispersion curve is subsequently visualized within the band structure diagram of figure7. This brand structure diagram shows the optical mode where two neighboring unit cells move out of phase and the acoustical mode where they move in phase [11]. A prominent feature of figure 7 is the existence of a distinct band gap for certain frequencies. This band gap is visible as a separation between the two curves which directly corresponds to the range where there is a negative effective mass according to relation 1.8. In essence, a negative effective mass in such a lattice system leads to the waves moving through the system becoming weaker [10]. It is noticeable that the location of the lower bound of the band gap is tied to the resonant frequency ($\frac{\omega}{\omega_0} = 1$). The resonant frequency, $\omega_0 = \sqrt{k_2/m_2}$, can be adjusted by changing the stiffness k_2 or the mass m_2.

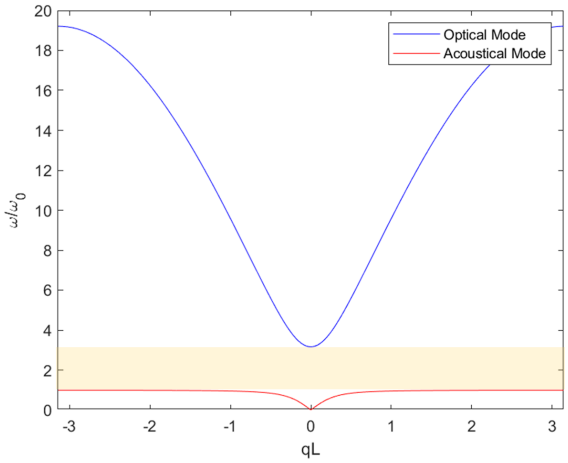

Figure 7: Nondimensionalized dispersion curve for the mass-in-mass lattice system

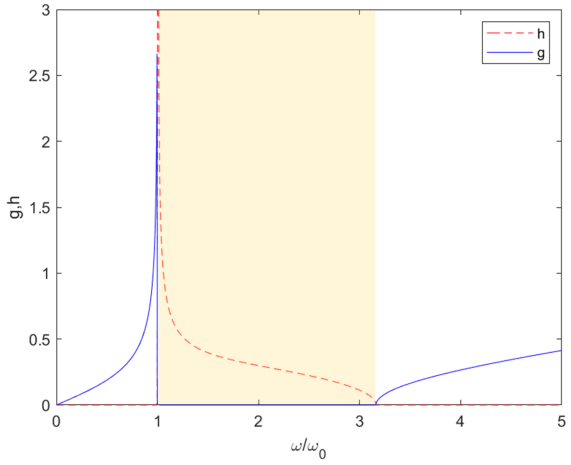

Figure 8: Nondimensionalized dispersion curve with complex wave number qL=g+ih

In figure 8 it is visible how the complex wave number changes with respect to the wave frequency. The wave number is dimensionless and presented as a complex number $qL = g + ih$. The real and imaginary part are separately shown in the plot.
The displacement is a function of e^{iqL}. By substituting $qL = g + ih$ into the wave solution, a relationship between the displacement and the complex wave number is established as:

$$u_\gamma \propto e^{i(g+ih)(x/L)} = e^{-h(x/L)} e^{ig(x/L)} \tag{3.8}$$

The term x/L represents a normalized spatial variable, where x denotes the relative spatial position with respect to the j^{th} unit cell.
It is observed that the amplitude of displacement is proportional to $e^{-h(x/L)}$. When the attenuation factor h takes a positive value, the wave number becomes purely imaginary, leading to a spatial displacement that decays exponentially. This attenuation effect is most pronounced when the frequency of the wave approaches the local resonance frequency ω_0. At the resonant frequency, the attenuation factor h, becomes unbounded and results in the maximum possible attenuation of the wave [4]. As the frequency of the wave gets closer to the end of the band gap, the wave's amplitude will continue to decrease until it eventually dissipates. This effectively illustrates the reduction of the wave within the band gap.

3.2 Negative effective mass

The dispersion curve of equation 3.4 is constructed considering the effective masses. This curve should align with the dispersion curve derived from the the mass in mass system equation 3.7). Given that the two curves need to be identical, it is possible to determine the effective mass, as the relationship between ω and qL must remain unchanged. Equation 3.4 can be used to validate this relationship. The equations need to be set equal to each other and solved for m_{eff}. Upon doing so, the following result for the effective mass is obtained:

$$m_{\text{eff}} = m_{\text{st}} + \frac{m_2 \left(\frac{\omega}{\omega_0}\right)^2}{1 - \left(\frac{\omega}{\omega_0}\right)^2} \tag{3.9}$$

In this equation $m_{st} = m_1 + m_2$ and represents the static mass. The dimensionless effective mass M_{eff}/m_{st} has been plotted as a function of ω/ω_o.

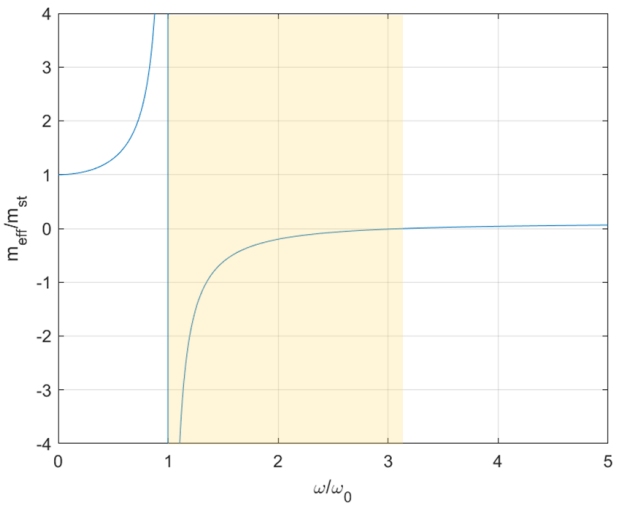

Figure 9: Dimensionless effective mass M_{eff}/m_{st} as function of ω/ω_0, with the marked box representing the band gap

The graph reveals some interesting features. After the local resonance frequency ω_0, the effective mass becomes negative. This is represented by a dip of the effective mass when it gets closer to the frequency ω_0. Also, at long wavelengths when ω approaches 0, the effective mass m_{eff} goes towards m_{st}, which is shown as the line becomes steady.

The occurrence of negative effective mass is interesting. Looking at equation 3.4, a negative effective mass is only possible when $1-\cos(qL)$ turns negative, implying that the dimensionless wave number (qL) is complex. When the effective mass is negative, the acceleration goes the opposite way to the force F. This makes the system's response amplitude U smaller. This is represented by a damping effect in the graph and verifiable with equation 1.1. The effective mass becomes positive again when the frequency exceeds $\omega/\omega_0 = \sqrt{m_2/m_1}$. The area where the effective mass is negative corresponds to the band gap, visualized as the marked area and belongs to the following frequency range:

$$1 < \frac{\omega}{\omega_0} < 1 + \frac{m_2}{m_1} \tag{3.10}$$

the size of this band gap corresponds to the band gap of the dispersion curve 7. In this specific frequency range, the metamaterial prevents the propagation of waves. The width of the band gap as inferred from equation 3.10 and figure 9 is related to the ratio of masses m_1 and m_2. It is apparent that increasing mass m_2 is helpful for the creation of a wider band gap.

4 Reflection in one dimensional finite LRAM system

In the exploration of wave propagation in a mass-in-mass lattice system, a good understanding of the dispersion relation and its implications on the system's behavior has been gained. The masses and stiffness of the springs from the system have been identified as crucial factors which influence the behavior of propagating waves within the lattice system. Furthermore the phenomenon of negative effective mass and its impact on wave propagation, leading to the formation of band gaps has also been observed.

When considering the case of ultrasound imaging , the propagation of waves involves a system composed of three distinct layers the skin, lLRAM coating and the needle. This multi-layered system introduces additional complexity when analyzing wave propagation. Each layer with its unique material properties, interacts differently with the incoming waves leading to different reflections and transmissions. Understanding these interactions give valuable insights on the way acoustic waves go through these layers and reflect off them.

The next chapter delves deeper into the principles of transmission and reflection of acoustic waves in layered media. When certain frequencies are prohibited from propagating in the lattice system due to the formation of band gaps, it is understood that waves are reflected back because they can't propagate through. By analysing how acoustic waves interact with the skin, LRAM, and needle, and with the understanding of dispersion plots and it's characteristics, the reflection magnitude can be determined and improved.

4.1 Reflection and transmission in a three layer setup

Layered media refers to structures composed of multiple layers, each with distinct material properties such as density and stiffness. These properties influence the transmission and reflection of acoustic waves. This understanding is crucial in fields like ultrasound imaging, where the interaction of acoustic waves with different layers can significantly impact the quality of the image.

One of the fundamental principles of acoustic waves going through different media is the conservation at an interface between the two media seen in figure 10. Which can be mathematically represented as:

$$p_i + p_r = p_t \tag{4.1}$$

where , p_i denotes the incident wave, which is the wave as it strikes the interface, p_r represents the reflected wave, or the wave that bounces back into the first medium, and p_t stands for the transmitted wave, which is the wave that passes through the interface into the second medium. The sum of the incident and reflected waves equals the transmitted wave of the interface. However, this is not always the case and can vary depending on whether dissipation is modeled or not. In the present work, dissipation is not included in the model.

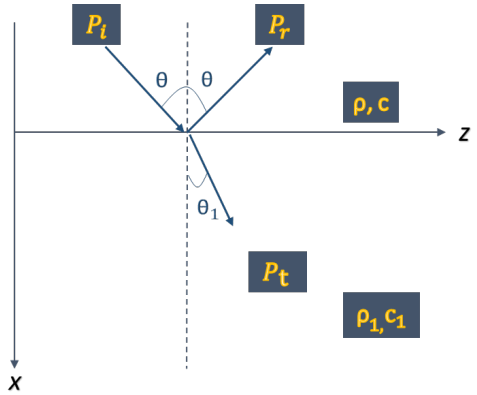

Figure 10: Transmission and reflection of acoustic waves at an interface between three media

To quantify the proportion of the incident wave that is reflected back from the interface, we use the reflection coefficient R, defined as:

$$R = \frac{p_r}{p_i} \tag{4.2}$$

This coefficient represents the ratio of the reflected wave to the incident wave. Similarly, the transmission coefficient T is used to quantify the proportion of the incident wave that is transmitted through the interface into the second medium:

$$T = \frac{p_t}{p_i} \tag{4.3}$$

By dividing each term of equation 4.1 by p_i, the equation can be reformulated as follow:

$$1 + R = T \tag{4.4}$$

4.2 Stress waves

Having understood the principles of reflection and transmission of sound waves at an interface, we can now delve deeper into the mathematical representation of these waves in 1D. It's important to note that when we talk about sound waves in a medium, we are actually talking about stress waves. This is because sound propagation in a material medium involves oscillation of the medium's particles due to the mechanical stress caused by the sound wave. Such mechanical stress results in compression and rarefaction within the medium, creating what is perceived as sound. The wave equation we will be using is specifically for these stress waves. The propagation of stress waves can be defined with a second-order linear partial differential equation, which is the one-dimensional wave equation given by:

$$\rho \frac{\partial^2 u_x}{\partial t^2} = \frac{\partial \sigma}{\partial x} \tag{4.5}$$

In this equation, ρ is the density of the medium, u_x is the horizontal displacement of a point in the medium, t is time, and σ is stress. This equation essentially describes how the displacement of a point in the medium changes over time due to the stress applied. The left-hand side of the equation represents the acceleration of a point in the medium (which is proportional to the force applied to it, according to Newton's second law), while the right-hand side represents the variation of stress (which is a measure of the force per unit area).

During the ultrasound imaging procedure, propagating waves traverse through three distinct layers. The sequence of the configuration is the skin, metamaterial and needle. As these waves reach the boundary interface between the skin and the metamaterial, a portion of the wave is transmitted into the metamaterial, while another part is reflected back. It's important to note that each of these transmitted and reflected waves carries its own stress.

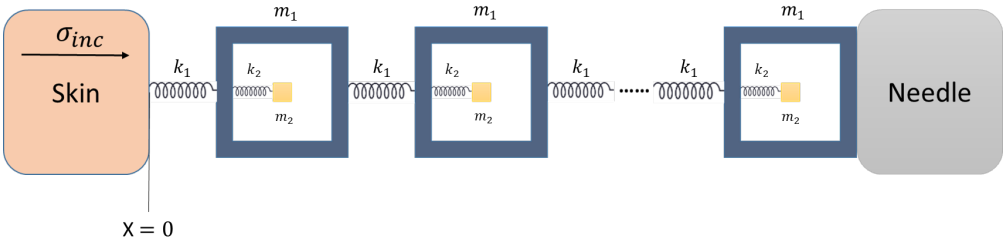

Figure 11: 1D representation of the metamaterial connected to the skin and needle

At the boundary $x = 0$, which is the interface between the skin and the metamaterial, the total stress σ is the sum of the incident stress σ_{inc} and the reflected stress σ_{ref}:

$$\sigma = \sigma_{inc} + \sigma_{ref} \tag{4.6}$$

This equation represents the boundary condition at the interface and provides a relationship between the incident and reflected stresses.

The derivative of stress with respect to position x, denoted as $\frac{d\sigma}{dx}$, can be expressed in terms of the time derivatives of the incident stress (σ_{inc}) and reflected stress (σ_{ref}), denoted as $\frac{d\sigma_{\text{inc}}}{dt}$ and $\frac{d\sigma_{\text{ref}}}{dt}$ respectively, each multiplied by the reciprocal of the wave speed c. This is represented as:

$$\frac{d\sigma}{dx} = -\frac{1}{c}\frac{d\sigma_{inc}}{dt} + \frac{1}{c}\frac{d\sigma_{ref}}{dt} \tag{4.7}$$

The reason this equality holds is due to the homogeneous nature of the material. In a homogeneous material, the wave speed is constant. This means that the rate of change of stress with respect to position ($\frac{d\sigma}{dx}$) is directly proportional to the rate of change of stress with respect to time ($\frac{d\sigma}{dt}$), with the constant of proportionality being the reciprocal of the wave speed ($\frac{1}{c}$).

By substituting the one-dimensional wave equation4.5 into equation 4.7 and integrating it over t, the relationship between the reflected stress σ_{ref} and the incident stress σ_{inc}, can be written as:

$$\sigma_{ref} - \sigma_{inc} = \rho c\frac{\partial u_1}{\partial t} \tag{4.8}$$

Therefore, the reflected stress can be expressed as:

$$\sigma_{ref} = \rho c\frac{\partial u_1}{\partial t} + \sigma_{inc} \tag{4.9}$$

The behavior of incident, reflected and transmitted waves have been explored, and the role of reflected stress has been understood. Now, the focus shifts to a key characteristic that governs these interactions called the acoustic impedance. This property denoted as Z, is a measure of a medium's resistance to the flow of sound energy. It is a function of the medium's density ρ and the speed of sound c within it. The impedance plays a critical role in determining how wave energy is partitioned at an interface between two media. It influences the amount of wave energy that is reflected back at the interface and the amount that is transmitted into the next medium.
In the upcoming section the calculation of acoustic impedance for the different materials the skin and the metamaterial will be delved into. And its role in determining the reflection coefficient, which quantifies the amount of the wave that is reflected back at an interface, will be examined.

4.3 Impedance

The configuration consists of three layers which is the skin connected to the metamaterial from one side and the needle on the other side. The skin and needle are semi-infinite and the metamaterial is finite. in figure 12 there is a schematic visualization of one wave hitting the interface of the skin and metmaterial. The transmitted waves and reflected waves are shown aswell. The total reflection is computed at the skin-metamaterial interface.

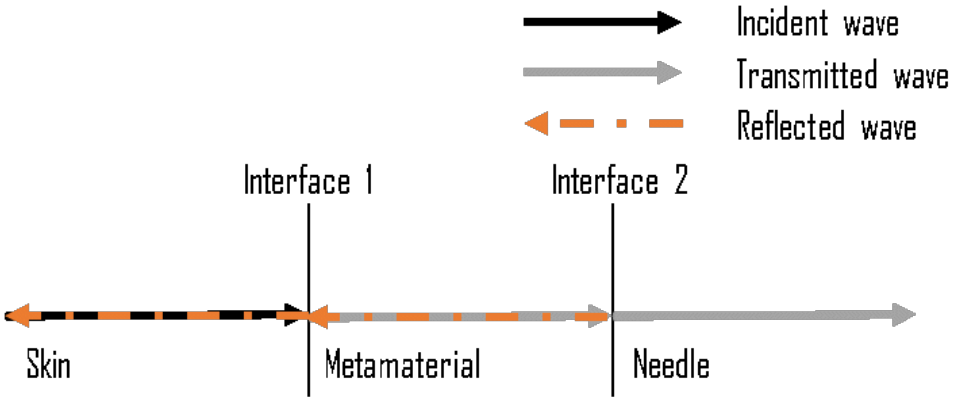

Figure 12: Schematic overview of a wave propagation through the three layered media

Acoustic impedance, denoted as Z, is a measure of how much a medium resists or impedes the flow of sound energy. In other words, it quantifies the opposition that a system presents to the acoustic wave. This resistance is due to the combined effects of the medium's density ρ and the speed of sound c within that medium. The impedance of a medium plays a crucial role in wave propagation as it influences the partitioning of wave energy at an interface between two media. Specifically, it determines the amount of wave energy that is reflected back at the interface and the amount that is transmitted into the next medium. Differences between the impedance's between layers cause reflection, and therefore the impedance can be used to compute the reflection.

The equation for calculating the acoustic impedance of the skin is given by [12]:

$$Z_1 = \frac{\rho_1 c_1}{\cos(\theta)} \tag{4.10}$$

Where θ represents the angle of incidence of the acoustic wave, ρ_1 is the density of the skin, and c_1 is the speed of sound in the skin. When the wave is at normal incidence (i.e., $\theta = 0$) of the interface, $cos(\theta)$ equals 1, simplifying the equation to $Z = \rho c$. The impedance of the metamaterial is denoted as Z_2. These two impedances, Z_1 and Z_2, of the skin and the metamaterial respectively, can be used to determine the reflection coefficient R [12].

$$R = \frac{Z_2 - Z_1}{Z_2 + Z_1} \tag{4.11}$$

The reflection coefficient R quantifies the amount of the wave that is reflected back at an interface between two media. If Z_1 and Z_2 are equal, the wave will pass through the interface without any reflection. However, if Z_1 and Z_2 are different, part of the wave will be reflected back into the first medium, and the rest will be transmitted into the second medium. The greater the difference between Z_1 and Z_2, the greater the proportion of the wave that will be reflected back.

When these waves encounter the interface of the skin and the metamaterial, both impedances Z_1 and Z_2 are required to compute the reflection coefficient. The skin, being a homogeneous material, allows for the use of equation 4.10 for this computation.
On the other hand, the metamaterial which has a mass-in-mass structure, presents a challenge. This structure results in a dynamic density that varies, making it difficult to compute the impedance using the same equation. In the case of a mass-in-mass structure, the system consists of smaller masses embedded within a larger mass. And it allows the smaller masses to move independently of the larger mass. The independent movement of the smaller masses can be influenced by factors such as resonance frequency. When the frequency of the incoming wave matches the natural frequency of the smaller masses, resonance occurs. This resonance can cause the smaller masses to oscillate at large amplitudes, leading to significant changes in the dynamic density of the metamaterial. However, there is another way to compute the impedance which is the ratio between the pressure $p_2(x = 0)$ and velocity $v_2(x = 0)$ of the wave at the boundary of the interface. The equation is given as [12]:

$$Z_{in} = \frac{p_2(x = 0)}{v_2(x = 0)} \tag{4.12}$$

So the pressure at the boundary interface between the skin and metamaterial is denoted as $p_2(x = 0)$. This is the pressure of the wave as it encounters the interface. The equation that holds for the total stress here is $\sigma = \sigma_{inc} + \sigma_{ref}$. However, as seen in equation 4.9 the reflected stress is $\sigma_{ref} = \rho c \frac{\partial u_1}{\partial t} + \sigma_{inc}$. And therefore the total stress becomes $2\sigma_{inc} + \rho_1 c_1 \frac{\partial u_1}{\partial t}$. It's important to note that in the context of waves, "stress" often refers to the force per unit area within materials that arises from externally applied forces, while "pressure" typically refers to the force exerted by a wave on the surface of an object. In this case, the pressure is working in the opposite direction to the stress, hence these quantities are negative.
The velocity at the boundary $v_2(x = 0)$, is equal to $\frac{\partial u_1}{\partial t}$.

The impedance of the metamaterial is then derived by taking the ratio of the pressure to the velocity at the boundary, as given by :

$$Z_2 = \frac{-2\sigma_{inc} + \rho_1 c_1 \frac{\partial u_1}{\partial t}}{\frac{\partial u_1}{\partial t}} \tag{4.13}$$

All the terms of the equation involving the pressure and velocity are either given or can be calculated except the velocity $v_2(x = 0)$ at the boundary interface. The density and speed of sound in the skin, ρ_1 and c_1 respectively, are physical properties that can be found in literature or measured experimentally. The incident stress, σ_{inc}, can be calculated from the amplitude of the incident wave A and the properties of the skin using the formula $\sigma_{inc} = \rho_1 c_1 A$. The unknown velocity $\frac{\partial u_1}{\partial t}$ can be computed by using the equation of motions.

4.4 Semi-analytical solution of the reflection coefficient

The equations of motion for a three-layered medium consisting of skin, metametamaterial and needle is needed to decribe the system. The system is designed in such a way that it is connected to just one unit cell of the skin and to one unit cell of the needle. In this context, a 'unit cell' refers to the smallest, repeatable unit of the structure that still retains the properties of the whole structure. The equation of motion for the material which is presented as a mass in mass lattice system is known.

Equation 4.9 for the reflected stress provides guidance in determining the forces at the interface of the skin and needle. The wave pressure at the interface of the skin is determined by the pressure applied from the skin to the metamaterial, it has been computed already in section 4.3 and resulted in $-2\sigma_{inc} + \rho_1 c_1 \frac{\partial u_1}{\partial t}$. It is important to note that the quantities in the definition of impedance, the pressure and stress, are measures of force per unit area. To obtain the total force , we must multiply by the surface area S, which represents the area of the coating hit by the wave. This results in the complete force being $(2\sigma_{inc} + \rho_1 c_1 \frac{\partial u_1}{\partial t})S$ for the incident wave onto the metamaterial.
The incident stress, denoted as σ_{inc}, is only applicable at the boundary interface where $x = 0$. Therefore the total stress for the needle interface can consequently be expressed as $\sigma_{ref} = \rho_3 c_3 \frac{\partial u_n}{\partial t}$, resulting in $\rho_3 c_3 \frac{\partial u_n}{\partial t} S$ for the force of the needle interface.

The equations of motion for the metamaterial are given by equations 3.5 and 3.6, which correspond to the outer and inner mass, respectively.
For the first unit cell u_1 at the boundary with the skin, and the last unit cell u_n which corresponds to the boundary with the needle, the equations of motion are as follow:

first unit cell u_1:
Outer mass:

$$m_1 \frac{\partial^2 u_1}{\partial t^2} = -(2\sigma_{inc} + \rho_1 c_1 \frac{\partial u_1}{\partial t})S - k(2u_1 - u_2) - k_R(u_1 - v_1) \tag{5.1}$$

inner mass:

$$m_2 \frac{\partial^2 v_1}{\partial t^2} = -k_R(v_1 - u_1) \tag{5.2}$$

last unit cell u_n:
outer mass:

$$m_1 \frac{\partial^2 u_n}{\partial t^2} = -\rho_3 c_3 \frac{\partial u_n}{\partial t} S - k(2u_n - u_{n-1}) - k_R(u_n - v_n) \tag{5.3}$$

inner mass:

$$m_2 \frac{\partial^2 v_n}{\partial t^2} = -k_R(v_n - u_n) \tag{5.4}$$

With the equations of motion for the skin, metamaterial, and needle established, a transition is made to a more generalized representation of these equations. This is achieved by expressing them in matrix form. This matrix representation is not just a mathematical convenience, but it also provides a more intuitive understanding of the system's behavior. Each matrix encapsulates a different aspect of the system, thereby facilitating the transformation of the system into a format that is helpful for analyzing the magnitude of the reflection .

The equations of motion hold the capability to be depicted as a second-order differential equation denoted as:

$$\mathbf{M}\frac{\partial^2 \mathbf{U}_j}{\partial t^2} + \mathbf{K}\mathbf{U}_j + \mathbf{G}\frac{\partial \mathbf{U}_j}{\partial t} + \mathbf{U}_{inc} = 0 \tag{5.5}$$

This second-order differential equation can be represented in a matrix form, where each matrix has its own unique role. The mass matrix, denoted as $\mathbf{M}$, signifies the mass contribution of the different unit cells in the lattice. The stiffness matrix represented by $\mathbf{K}$, embodies the rigidity of the system. The acoustic impedance of the skin and needle interface is represented in matrix $\mathbf{G}$. Lastly, $\mathbf{U}_{inc}$ represents the incident stress.

The mass matrix of a single unit cell contains properties of both the outer and inner mass. For the normalization of the matrix corresponding to one unit cell, denoted as $\mathbf{M_{unit}}$, the term $\beta = \frac{m_2}{m_1}$ is utilized. This leads to the derivation of the resulting matrix for a unit cell.

$$\mathbf{M}_{\text{unit}} = \begin{bmatrix} 1 & 0 \\ 0 & \beta \end{bmatrix} \tag{5.6}$$

The mass matrix $\mathbf{M}$, is a summation of the mass matrices of all unit cells, with n representing the number of unit cells in the lattice.

$$M = \sum_{e=1}^{n} m_{\text{unit}} \tag{5.7}$$

The stiffness matrices for the unit cells differ because they are located at different positions, and hence, the influence of the springs varies. The normalization of the stiffness is achieved using the term $\alpha = \frac{k_2}{k_1}$. Subsequently, the corresponding matrices for each unit cell are derived. .

$$\begin{aligned} K_1 &= \begin{bmatrix} 1+\alpha & -\alpha & -1 \\ -\alpha & \alpha & 0 \end{bmatrix} \\ K_{\text{j}} &= \begin{bmatrix} -1 & 2+\alpha & -\alpha & -1 \\ 0 & -\alpha & \alpha & 0 \end{bmatrix} \quad \text{for } j = 2, ..., n-1 \\ K_{\text{n}} &= \begin{bmatrix} -1 & 1+\alpha & \alpha \\ 0 & -\alpha & \alpha \end{bmatrix} \end{aligned} \tag{5.8}$$

Matrix $\mathbf{G}$ is only relevant for first and last unit cell because impedance only applies to these two unit cells. This term is normalized by $\gamma_i = \rho_i \times c_i$, where i is 1 for the first unit cell and n for the last unit cell. Also $L = \frac{m}{{l_m}^2}$ is used, where ${l_m}^2$ is S the lateral surface. Matrix G is presented as:

$$G = \begin{bmatrix} \frac{\gamma_1 l^2 m}{\sqrt{km}} & 0 & \cdots & 0 \\ 0 & 0 & \cdots & 0 \\ \vdots & \vdots & \ddots & \vdots \\ 0 & 0 & \cdots & \frac{\gamma_n l^2 m}{\sqrt{km}} \end{bmatrix} \tag{5.9}$$

Introducing two new terms: $\tau = \omega t$ and $\Omega = \frac{\omega}{\omega_0}$, leads to a normalized second-order differential equation.

$$\mathbf{M}\Omega^2 \frac{\partial^2 \mathbf{U}_j}{\partial \tau^2} + \mathbf{K}\mathbf{U}_j + \mathbf{G}\Omega \frac{\partial \mathbf{U}_j}{\partial \tau} + \mathbf{U}_{inc} = 0 \tag{5.10}$$

Eventually the unknown $\frac{\partial U_j}{\partial \tau}$ can be solved from equation 5.10 with help of a general solution in the form of :

$$\tilde{C} = [1, C_2 \cos(-\tau), C_3 \sin(-\tau)] \tag{5.11}$$

This vector represents a set of solutions to the normalized second-order differential equation. In order to use it for the system a matrix is required and therefore S is introduced. S is a special kind of matrix. It's constructed by taking an identity matrix (with size matching the number of unit cells) and multiplying each of its elements by the corresponding element from the transpose of $\tilde{C}$.

$$S = I_n \otimes C^T \tag{5.12}$$

This process is known as projection, and used to transform the system into a simpler form for determining the values of the solution vector. For each single term from the second order differential, S is substituted and all terms are multiplied by the transpose of S.

$$\begin{aligned} A_1 &= S^T \mathbf{M} \frac{d^2 S}{dt^2} & C_1 &= S^T \mathbf{K} S \\ B_1 &= S^T \mathbf{G} \frac{dS}{dt} & DD_1 &= S^T S \mathbf{U}_{inc} \end{aligned} \tag{5.13}$$

The results are integrated over one period and normalized by dividing by π to get the average value for the matrices A and B respectively. A represents the behavior due to the masses, stiffness and resistance at the boundary, while B describes the influence of the incident stress.

$$A = \frac{1}{\pi} \int_0^{2\pi} (\omega^2 A_1 + \omega B_1 + C_1)\, dt, \qquad B = -\frac{1}{\pi} \int_0^{2\pi} DD_1\, dt \tag{5.14}$$

Given the matrices A and B, the objective is to solve for the vector X, which contains the coefficients of the solution. For the system to be in equilibrium, the external force exerted by the incident stress must be balanced by the internal forces generated by the system's current state and therefore it holds:

$$AX = B \tag{5.15}$$

after all the coefficients of X are found through the application of a linear equation.

$$X = A^{-1} B \tag{5.16}$$

The variables corresponding to the the second and third element of the solution vector are C_2 and C_3 , which correspond to $\cos(-\tau)$ and $\sin(-\tau)$ respectively. Substituting the solution of the term $\frac{\partial U}{\partial \tau}$ into the equation for the reflection coefficient as $(C_2 + C_3)$ yields the reflection coefficient for a given incident frequency.

As described in equation 4.11. The reflection magnitude denoted by $|R|$ and is given by:

$$R = \frac{\left(\frac{-2\sigma_{\text{inc}} + \rho_1 c_1 \frac{\partial u_1}{\partial t}}{\frac{\partial u_1}{\partial t}} \right) - \rho_1 c_1}{\left(\frac{-2\sigma_{\text{inc}} + \rho_1 c_1 \frac{\partial u_1}{\partial t}}{\frac{\partial u_1}{\partial t}} \right) + \rho_1 c_1} \tag{5.17}$$

To analyze the reflection coefficient of the system, the equation of the reflection magnitude is normalized. This normalization process uses terms defined in the previous section. After normalization, a new equation for the reflection coefficient is obtained, which is given by:

$$R = \frac{-\Omega \gamma_1 l^2 m \frac{\partial u}{\partial \tau}}{\sqrt{km}} + 1 \tag{5.18}$$

The absolute value is taken in order to have the reflection magnitude $|R|$.

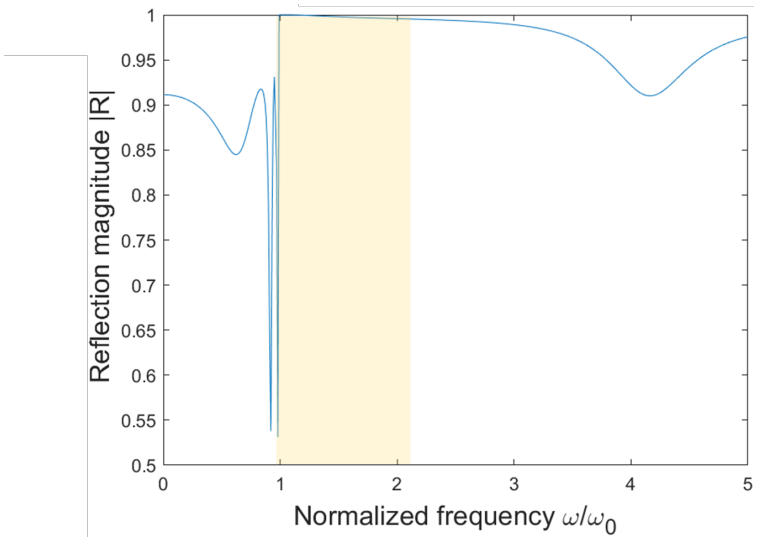

Figure 13: Reflection magnitude $|R|$ vs Normalized frequency

In the graphical representation of figure 13, the x-axis represents the normalized frequencies($\frac{\omega}{\omega_0}$) , while the y-axis denotes the reflection magnitude $|R|$. The normalized frequency of 1 which is the resonance frequency is the starting point of the band gap. The end of the band gap is given by equation 3.10, thereby the total range for the band gap is illustrated by the marked rectangle. The start of the band gap is shown by the reflection magnitude reaching a value of 1, which indicates that waves are not propagating through the material but are instead being reflected back. It is visible that the reflection magnitude is equal or nearly 1 within the range of the band gap. This observation supports the theoretical understanding that wave propagation is inhibited within the band gap.
Based on the theory of the band gap and the associated parameters like mass and stiffness ratio, it is now possible to examine the reflection magnitude $|R|$. By adjusting these parameters and studying the subsequent changes in both the band gap and the reflection magnitude, the effects can be observed. Changes in the width of the band gap, and the range of frequencies where the reflection magnitude is equal to 1 are of interest, since these dictate the reflection of the LRAM.

5 Parametric analysis

The parametric analysis involves an examination of parameters that influence reflection. Initially, the individual effects of the mass ratio $\beta = \frac{m_2}{m_1}$ and the stiffness ratio $\alpha = \frac{k_2}{k_1}$ on reflection performance are analyzed. Following this, a combined effect is studied by simultaneously altering both α and β. The analysis also takes into account the number of unit cells, given its significance in determining the thickness of the coating.

First, the influence of increasing the mass ratio $\beta = \frac{m_2}{m_1}$ will be investigated. Figure 14a illustrates the reflection magnitude for varying values of β as a function of $\frac{m_2}{m_1}$, the frequency normalized by the resonance frequency corresponding to the reference design β, is used across all variations.
The start of the band gap is clearly shown at the point where the reflection coefficient reaches 1. The end of the band gap is less apparent, but can be obtained from the dispersion curve (7), and is indicated by a color-corresponding dashed vertical line.

Upon increasing β, it was noted that the end of the band gap exhibits a minimal shift, while the local resonance marking the start of the band gap decreases. This observation aligns with the resonance formula $\omega_0 = \sqrt{k_2/m_2}$, because an increase in the mass ratio β is equivalent to an increase in m_2 for the resonator.

Despite the increase in the width of the band gap, it is evident from figure 14b that the reflection magnitude does not improve by increasing parameter β, given by the fact that the reflection magnitude doesn't reach 1 for a bigger frequency range.
An examination of the behavior of the different waves before the band gap indicates a consistent number of dips preceding the resonance frequency with an increasing β. .
A conclusion drawn from the observations confirms that an increase of the the inner mass m_2, thereby increasing β indeed results in a wider band gap.

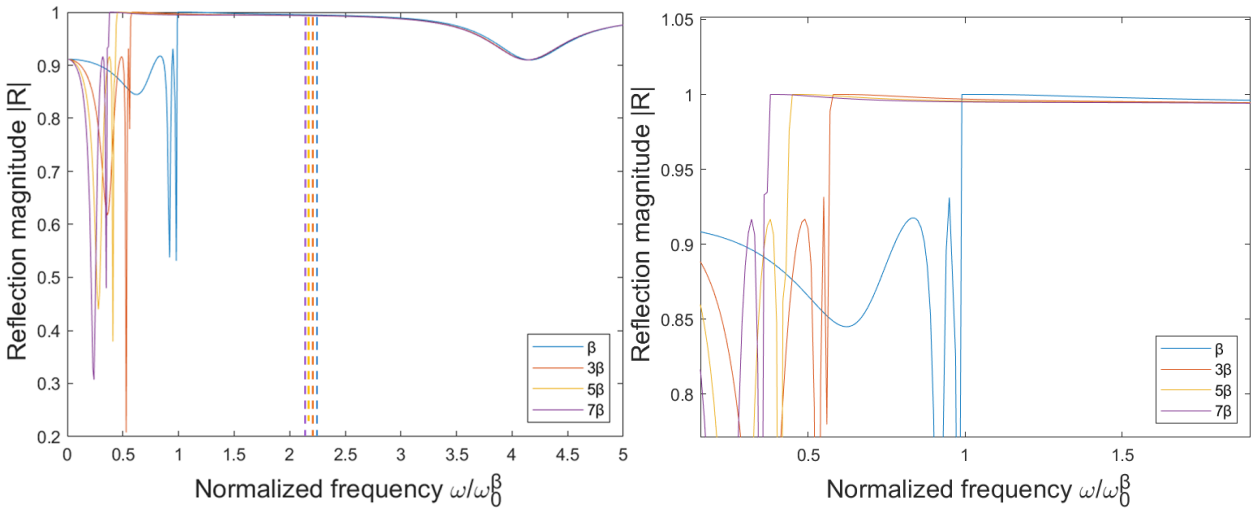

(a) Reflection magnitude $|R|$ vs normalized frequency

(b) Close-up view of the reflection magnitude $|R|$

Figure 14: Reflection magnitude $|R|$ vs normalized frequency with varying $\beta(\frac{m_2}{m_1})$

Next, the investigation will focus on the influence of the spring constant ratio, $\alpha = \frac{k_2}{k_1}$, on the reflection performance. For the purpose of this investigation, the other parameters are held constant.
The plot of figure 15a represents the reflection magnitude as a function of frequency, which has been normalized by the local resonance of the reference design α.
Upon examining the resonance frequency, it becomes evident that an increase in α increases the resonance frequency. This observation is consistent with the resonance formula $\omega_0 = \sqrt{k_2/m_2}$, because an increase in the stiffness ratio α is equivalent to an increase in k_2.

.
Furthermore, the end of the band gap appears to shift up more significantly, leading to a wider band gap.

An improvement in the reflection magnitude is also noticeable, as can be seen from figure 15b. This is clearly visible as the reflection magnitude stays closer to 1 for an extended range. The amplitude of the dips observed before the local resonance decreases when increasing α. The reason for this is the increase of the stiffness k_2, which makes the resonator stiffer and leads to less energy being stored just before the local resonance.
After the band gap, the dips exhibit similar behavior and shift accordingly. The amplitude of the dips don't change after the band gap because the waves are no longer in resonance with the system, and therefore the material properties have less influence.
After all, from these observations, it can be concluded that the reflection improves with an increase in α.

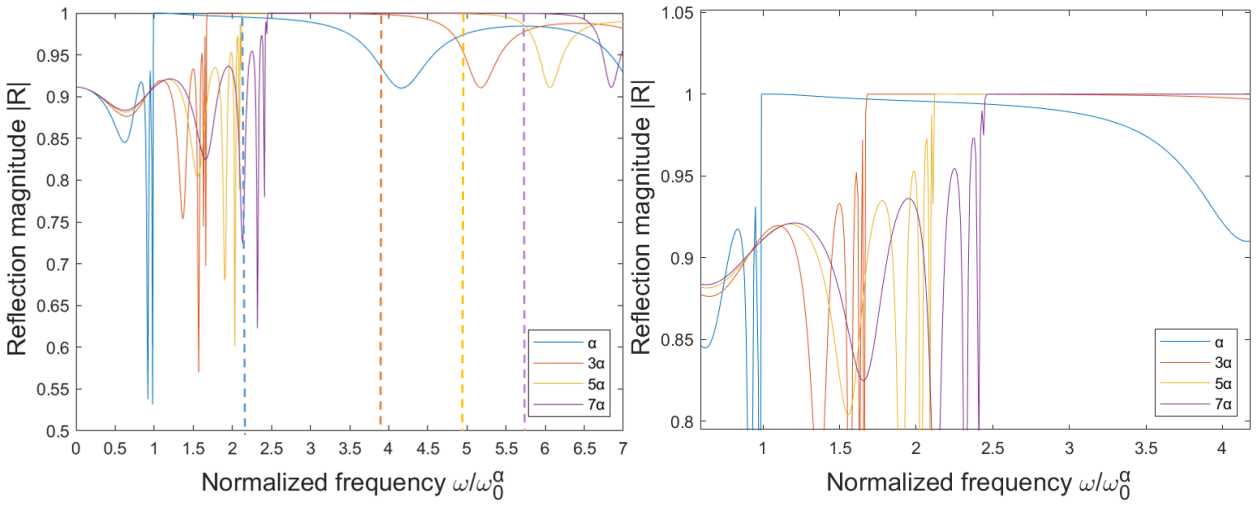

(a) Reflection magnitude $|R|$ vs normalized frequency

(b) Close-up view of the reflection magnitude $|R|$

Figure 15: Reflection magnitude $|R|$ vs normalized frequency with varying $\alpha(\frac{k_2}{k_1})$

Subsequently, the influence of both α and β on the reflection performance will be investigated.
The plot in figure 16 depicts the reflection magnitude as a function of frequency, normalized by the local resonance of the reference design α, β. The values for β and α increase equivalently, implying that the resonant frequency remains constant. This observation is confirmed by the resonance formula, which remains constant, given that both variables change proportionally.
It is evident from figure 16 that the band gap indeed enlarges for an increasing α and β. Additionally, the reflection magnitude is 1 for an expanded range of frequencies within the band gap.
The amplitude of the dips before the band gap seems to increase for an increasing α and β. In this case the stored energy of an increasing mass m_2 is transferred efficient by the increasing stiffness k_2 ,which leads to a consistent increase in the amplitude.
Eventually it can be inferred that an increase in both the mass ratio β and the stiffness ratio α results in an improvement of the reflection.

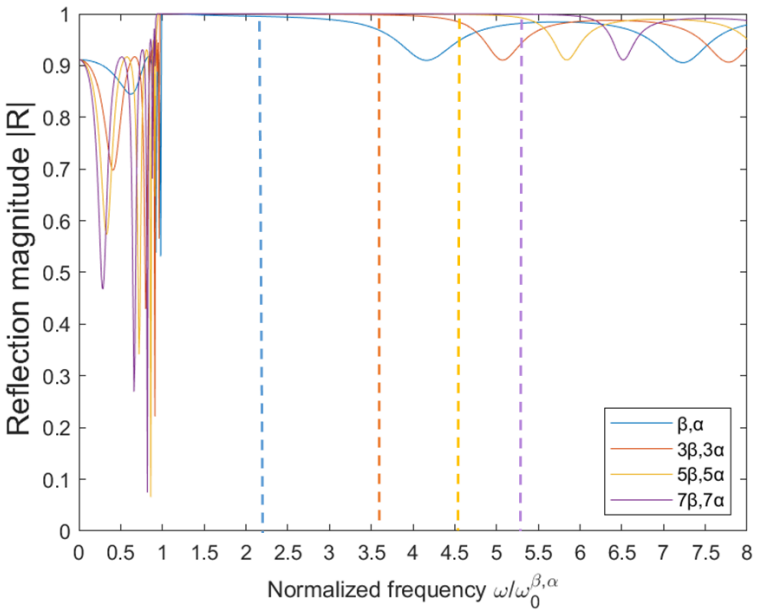

Figure 16: Reflection magnitude $|R|$ vs normalized frequency with a variation of β and α

Lastly, the influence of the number of unit cells will be investigated. This parameter is significant as it determines the thickness of the LRAM coating. The plot of figure 17a illustrates the reflection magnitude as a function of the normalized frequency.
For this analysis, the other parameters are held constant. The local resonance and band gap remain unchanged, which is expected as the material properties are not altered.

In figure 17a, two systems with 5 and 9 unit cells are constructed, and a comparison is made with the original system, containing 7 unit cells.
While the band gap remains constant, a close-up view of the reflection magnitude (figure 17b) reveals that within the band gap, the reflection magnitude is 1 for a wider range of frequencies for 9 unit cells. This is because in an LRAM, each unit cell interacts with the incoming acoustic wave, causing a portion of it to be reflected. When there are more unit cells, the incoming wave encounters more of these interactions, leading to a cumulative increase in the overall reflection. This indicates that the reflection magnitude can be enhanced by increasing the amount of unit cells.

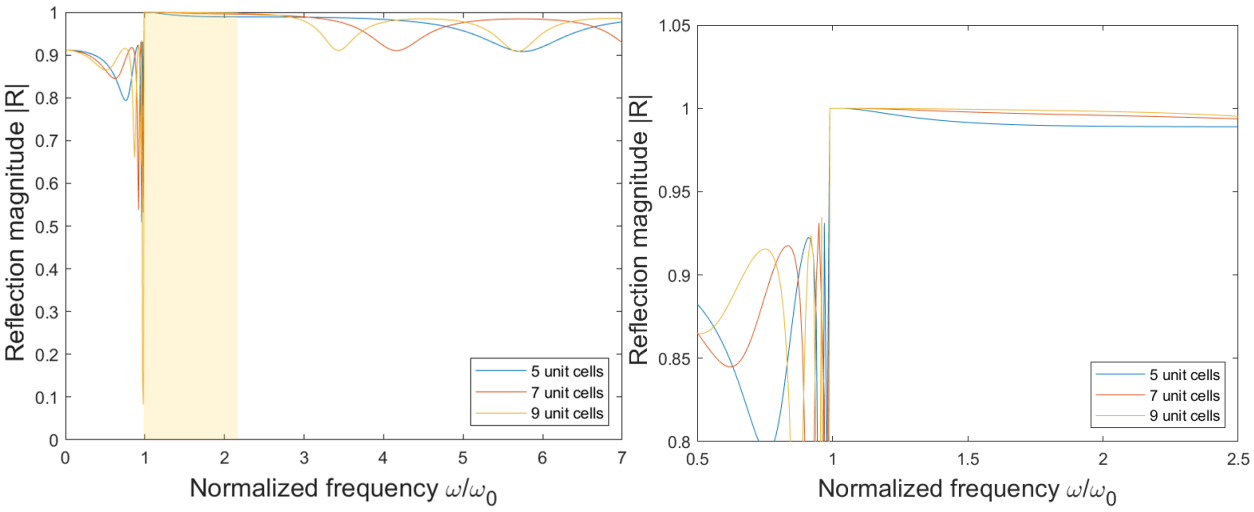

(a) Reflection magnitude $|R|$ vs normalized frequency

(b) Close-up view of the reflection magnitude $|R|$

Figure 17: Reflection magnitude $|R|$ vs normalized frequency with varying amount of unit cells

As the number of unit cells increases, so does the number of dips observed in figure 17a after the band gap. This is visible as the system with 9 unit cells already presents two distinct dips after the band gap within the visible range. Meanwhile, the system with 5 unit cells only exhibits one dip. This is a result of the interaction between the incident and reflected waves. In a wave, the peak is the highest point, while the trough is the lowest point. These represent the maximum upward and downward movements of the wave from its equilibrium. When two waves meet and their peaks and troughs do not align, they partially or completely cancel each other out, leading to a dip in the reflection magnitude. However, when the two waves meet and their peaks and troughs align , they combine to form a larger wave resulting in an increase in the reflection magnitude. Therefore, as the amount of unit cells increases it can accommodate a greater number of standing waves, thereby increasing the number of observable dips.

To summarize, the band gap's width is influenced by the mass ratio β and the stiffness ratio α. Specifically, an increase of the inner mass m_2 increases β, which subsequently widens the band gap. Similarly, a higher stiffness ratio α expands the band gap.
Furthermore, it is observed that the reflection magnitude within the band gap can be optimized by increasing the stiffness ratio α. Increasing α results in the reflection magnitude being 1 for wider range within the band gap. A similar improvement of the reflection magnitude within the band gap is achieved by increasing the number of unit cells, although this parameter does not influence the size of the band gap.
Increasing β and α simultaneously both increases the size of the band gap and improves the reflection magnitude within this range.

6 Conclusion and recommendations

This research undertook a comprehensive study in one dimension on the reflection magnitude of a locally resonant acoustic metamaterial (LRAM) coating. The primary objective was to enhance the reflection of a needle during ultrasound imaging procedures, a crucial factor that can significantly influence the success and safety of such procedures. The two main criteria investigated were the reflection magnitude and the band gap.

The research commenced with an exploration of the composition and structure of the LRAM coating. The composite structure of the LRAM, comprising heavy inclusions with a compliant layer in a matrix, was described in a 1D discrete model. Examination of a single unit cell unveiled the phenomenon of the effective mass, which can stop wave propagation when it turns negative.
The dispersion relation showed the relationship between the wave number and the frequency, and provided insights into the location of the resonance frequency and the band gap. The imaginary part of the complex wave number demonstrated how the wave attenuates within the band gap. Furthermore, the location of the band gap was confirmed by the negative effective mass within the band gap.
Upon understanding the principles of the band gap, the subsequent step was to compute the reflection coefficient for the system. Initially, the fundamental principles of transmission and reflection between media were observed, and the acoustic waves were described as stress waves. The reflected stress was expressed and utilized to determine the equations of motion of the boundary unit cells corresponding to the skin and needle, respectively.
The equations of motion for the discrete mass-in-mass system were then employed to describe the system with matrices and a second-order differential equation. A general solution was projected in order to transform the system, and it made it possible to solve a linear equation for the coefficients, for the reflection .
Ultimately, a parametric analysis was conducted. The influence of relevant parameters on the reflection magnitude and band gap was investigated. The findings revealed that increasing the mass ratio (β) and stiffness ratio (α) simultaneously both enhances the band gap and the reflection magnitude. Only increasing β improves the band gap, while increasing α individually improves both the band gap and reflection magnitude. Also increasing the number of unit cells results in an improvement of the reflection magnitude.

This research has demonstrated that the reflection of the needle's coating is dependent on the internal structure of the LRAM. The subsequent step would be to approach this problem in two dimensions. Since this system did not consider shear stresses, which are relevant when approaching the system in 2D, this could alter the system's behavior and consequently the results.

References

[1] C. Eder, "Medical devices with ultrasound-guided navigation ease needle placement for healthcare professionals", May 2017.

[2] Z. Liu, X. Zhang, Y. Mao, Y. Y. Zhu, Z. Yang, C. T. Chan, and P. Sheng, "Locally resonant sonic materials", *Science*, vol. 289, no. 5485, pp. 1734-1736, 2000.

[3] Z. Liu, C. T. Chan, and P. Sheng, "Three-component elastic wave band-gap material", *The American Physical Society*, vol. 65, 2002.

[4] B.S. Lazarov, J.S. Jensen, "Low-frequency band gaps in chains with attached with non-linear oscillators", *Int. J. Non-linear Mech.*, vol. 42, pp. 1186–1193, 2007.

[5] P. Sheng, J. Mei, Z. Liu, and W. Wen, "Dynamic mass density and acoustic metamaterials", *Science*, vol. 394, pp. 256-261, 2007.

[6] P. Sheng, X. Zhang, Z. Liu, and C. Chan, "Locally resonant sonic materials", *Elsevier*, vol. 338, pp. 201-205, 2003.

[7] G. Milton and J. Willis, "On modifications of Newton's second law and linear continuum elastodynamics", *Proceedings of the Royal Society A*, vol. 463, pp. 855-880, 2007.

[8] H. Huang and C. Sun, "Wave attenuation mechanism in an acoustic metamaterial with negative effective mass density", *New Journal of Physics*, vol. 11, 2009.

[9] S. Yao, X. Zhou, and G. Hu, "Experimental study on negative effective mass in a 1D mass-spring system", *New Journal of Physics*, vol. 10, 2008.

[10] H.H. Huang, C.T. Sun, and G.L. Huang, "On the negative effective mass density in acoustic metamaterials", *International Journal of Engineering Science*, vol. 47, pp. 610–617, 2009.

[11] P.K. Misra, "§2.1.3 Normal modes of a one-dimensional chain with a basis", *Physics of Condensed Matter*, Academic Press, p. 44, 2010.

[12] L.M. Brekhovskikh, "Waves in Layered Media", *Applied Mathematics and Mechanics*, Second Edition, Translated by R.T. Beyer, Department of Physics, Brown University, Providence, Rhode Island, Published by Academic Press, Inc., New York, London, Toronto, Sydney, San Francisco, 1980.

A Appendix

A.1 Material properties Lram

Material	Epoxy Matrix	Rubber	Tungsten
Density (kg/m^8)	900	1100	19300
Young's Modulus (Pa)	0.5×10^9	0.01×10^9	400×10^9
Longitudinal Velocity (m/s)	7.45×10^2	30.15	4.55×10^3

A.1.1 Geometry LRAM

Geometry	Epoxy Matrix	Rubber	Tungsten
Length (m)	4.5×10^-6	0.5×10^-6	0.5×10^-6
Volume (m^8)	7.69×10^-17	9.948×10^{-18}	4.19×10^-18
Area (m^2)	1.32×10^-11	3.93×10^-12	3.14×10^-12

A.2 Material Properties Skin and Needle

Material	Skin	Needle (Stainless Steel)
Density (kg/m^8)	1090	8000
Young's Modulus (Pa)		180×10^9
Longitudinal Velocity (m/s)	1615	4.74×10^3

A.3 Properties mass and spring

Mass	Mass(kg)
Main mass (matrix+coating) m_1	6.93×10^{-14}
Mass of attached resonator m_2	2.89×10^{-13}

Spring	Stiffness (N/m)
Main chain (matrix material) k_1	4.39×10^3
Attached resonator (coating) k_2	3.93